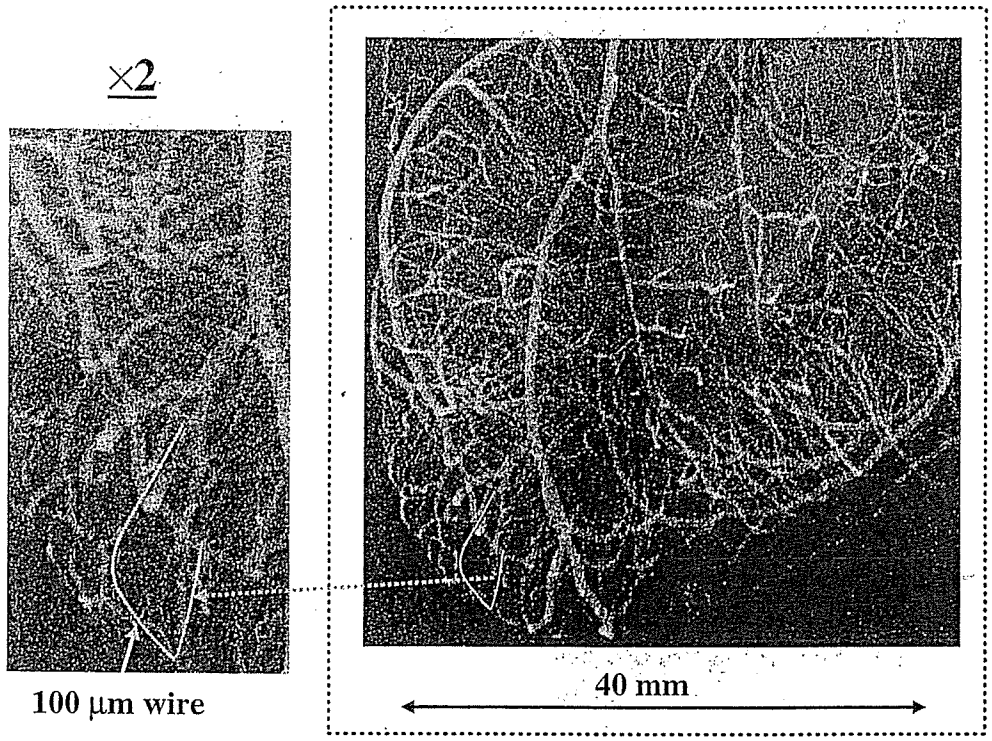

Fig. 8. Angiogram of extracted dog heart in 100-mm-thick water phantom using iodine microspheres.

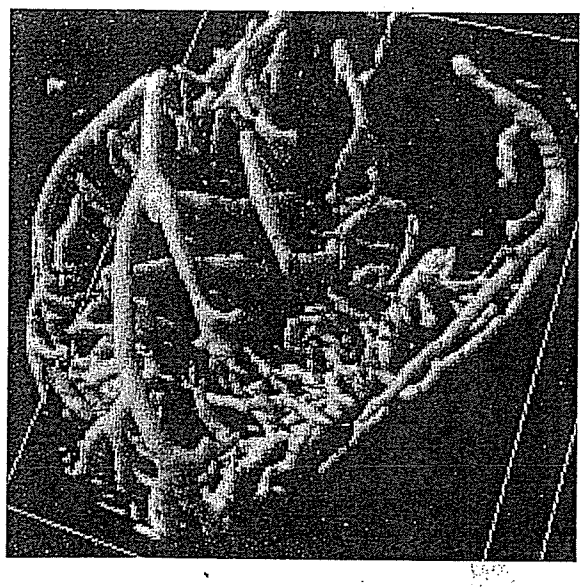

Fig. 9. Three-dimensional image of coronary arteries constructed from X-ray CT images taken by Pascal.

without filtering. Using the filter to absorb Kβ and bremsstrahlung X-rays, Kα rays were left, and we performed K-edge angiography using the filter with a tube voltage of 60 kV. To produce clean characteristic X-rays without using the filter, the angle dependence of the bremsstrahlung intensity should be considered, since bremsstrahlung rays are not emitted in the direction opposite that of the electron trajectory in Sommerfeld's theory.[18]

Currently, angiography is performed using both the bremsstrahlung and characteristic X-rays produced from a tungsten X-ray tube. However, enhanced K-edge angiography in this work was primarily performed using cerium Kα rays. Using the filter, the maximum number of Kα photons was approximately 3×10^7 photons/(cm^2·s) at 1.0 m from the source, and the photon count rate can be increased easily by improving the target. For example, a new rotation anode tube has been designed to increase the X-ray dose rate, and the rate can be increased by increasing the anode diameter.

In energy-selective imaging including K-edge angiography, the filtering effect of the absorber should be considered, and the X-ray spectra using the filter at a tube voltage of 60 kV hardly varies with changes in the thickness of the water phantom according to the spectrum estimation. Due to the absorption coefficient, Kβ rays are also useful for angiography, and both the Kα and Kβ rays can be left using a cerium oxide filter with a surface density of approximately 10 mg/cm^2. In addition, an aluminum filter with a thickness of approximately 3.0 mm is useful in absorbing unnecessary bremsstrahlung X-rays with energies lower than the K-absorption edge.

Acknowledgment

This work was supported by Grants-in-Aid for Scientific Research (13470154, 13877114, 16591181, and 16591222) and Advanced Medical Scientific Research from MECSST, Health and Labor Sciences Research Grants (RAMT-nano-001, RHGTEFB-genome-005 and RHGTEFB-saisei-003), Grants from the Keiryo Research Foundation, The Promotion and Mutual Aid Corporation for Private Schools of Japan, Japan Science and Technology Agency (JST), and the New Energy and Industrial Technology Development Organization (NEDO, Industrial Technology Research Grant Program in '03).

1) A. Akisada, M. Ando, K. Hyodo, S. Hasegawa, K. Konishi, K. Nishimura, A. Maruhashi, F. Toyofuku, A. Suwa and K. Kohra: Nucl. Instrum. Methods Phys. Res., Sect. A **246** (1986) 713.
2) A. C. Thompson, H. D. Zeman, G. S. Brown, J. Morrison, P. Reiser,

V. Padmanabahn, L. Ong, S. Green, J. Giacomini, H. Gordon and E. Rubenstein: Rev. Sci. Instrum. **63** (1992) 625.
3) H. Mori *et al.*: Radiology **201** (1996) 173.
4) K. Hyodo, M. Ando, Y. Oku, S. Yamamoto, T. Takeda, Y. Itai, S. Ohtsuka, Y. Sugishita and J. Tada: J. Synchrotron Radiat. **5** (1998) 1123.
5) T. J. Davis, D. Gao, T. E. Gureyev, A. W. Stevenson and S. W. Wilkims: Nature **373** (1995) 595.
6) A. Momose, T. Takeda, Y. Itai and K. Hirano: Nat. Med. **2** (1996) 473.
7) M. Ando, A. Maksimenko, H. Sugiyama, W. Pattanasiriwisawa, K. Hyodo and C. Uyama: Jpn. J. Appl. Phys. **41** (2002) L1016.
8) E. Sato, S. Kimura, S. Kawasaki, H. Isobe, K. Takahashi, Y. Tamakawa and T. Yanagisawa: Rev. Sci. Instrum. **61** (1990) 2343.
9) A. Shikoda, E. Sato, M. Sagae, T. Oizumi, Y. Tamakawa and T. Yanagisawa: Rev. Sci. Instrum. **65** (1994) 850.
10) K. Takahashi, E. Sato, M. Sagae, T. Oizumi, Y. Tamakawa and T. Yanagisawa: Jpn. J. Appl. Phys. **33** (1994) 4146.
11) E. Sato, K. Takahashi, M. Sagae, S. Kimura, T. Oizumi, Y. Hayasi, Y. Tamakawa and T. Yanagisawa: Med. Biol. Eng. Comput. **32** (1994) 289.
12) E. Sato, Y. Hayasi, R. Germer, E. Tanaka, H. Mori, T. Kawai, T. Ichimaru, K. Takayama and H. Ido: Rev. Sci. Instrum. **74** (2003) 5236.
13) E. Sato, Y. Hayasi, R. Germer, E. Tanaka, H. Mori, T. Kawai, T. Ichimaru, S. Sato, K. Takayama and H. Ido: J. Electron Spectrosc. Relat. Phenom. C **137–140** (2004) 713.
14) E. Sato, Y. Hayasi, R. Germer, E. Tanaka, H. Mori, T. Kawai, H. Obara, T. Ichimaru, K. Takayama and H. Ido: Jpn. J. Med. Phys. **20** (2003) 123.
15) E. Sato, E. Tanaka, H. Mori, T. Kawai, T. Ichimaru, S. Sato, K. Takayama and H. Ido: Med. Phys. **32** (2005) 49.
16) E. Sato, E. Tanaka, H. Mori, T. Kawai, T. Ichimaru, S. Sato, K. Takayama and H. Ido: Med. Phys. **31** (2004) 3017.
17) E. Sato, K. Sato and Y. Tamakawa: Annu. Rep. Iwate Med. Univ. School Lib. Arts Sci. **35** (2000) 13.
18) B. K. Agarwal: *X-ray Spectroscopy* (Springer-Verlag, New York, 1991) 2nd ed., p. 18.

Energy-selective high-speed radiography utilizing stroboscopic x-ray generator

Eiichi Sato*[a], Etsuro Tanaka[b], Hidezo Mori[c], Toshiaki Kawai[d], Shigehiro Sato[e], Hidenori Ojima[f], Kazuyoshi Takayama[f] and Hideaki Ido[g]

[a] Department of Physics, Iwate Medical University, 3-16-1 Honchodori, Morioka 020-0015, Japan
[b] Department of Nutritional Science, Faculty of Applied Bio-science, Tokyo University of Agriculture, 1-1-1 Sakuragaoka, Setagaya-ku, 156-8502, Japan
[c] Department of Cardiac Physiology, National Cardiovascular Center Research Institute, 5-7-1 Fujishirodai, Suita, Osaka 565-8565, Japan
[d] Electron Tube Division #2, Hamamatsu Photonics K. K., 314-5 Shimokanzo, Toyooka Village, Iwata-gun 438-0193, Japan
[e] Department of Microbiology, School of Medicine, Iwate Medical University, 19-1 Uchimaru, Morioka 020-8505, Japan
[f] Shock Wave Research Center, Institute of Fluid Science, Tohoku University, 2-1-1 Katahira, Sendai 980-8577, Japan
[g] Department of Applied Physics and Informatics, Faculty of Engineering, Tohoku Gakuin University, 1-13-1 Chuo, Tagajo 985-8537, Japan

ABSTRACT

Energy-selective high-speed radiography utilizing a kilohertz-range stroboscopic x-ray generator and its application to high-speed angiography are described. This generator consists of the following major components: a main controller, a condenser unit with a Cockcroft-Walton circuit, and an x-ray tube unit in conjunction with a grid controller. The main condenser of about 500 nF in the unit is charged up to 100 kV by the circuit, and the electric charges in the condenser are discharged to the triode by the grid control circuit. Although the tube voltage decreased during the discharging for generating x rays, the maximum value was equal to the initial charging voltage of the main condenser. The maximum tube current and the repetition rate were approximately 0.5 A and 32 kHz, respectively. The x-ray pulse width ranged from 0.01 to 1.0 ms, and the maximum shot number had a value of 32. At a charging voltage of 80 kV and a width of 1.0 ms, the x-ray intensities obtained without filtering, using an aluminum filter, and using a barium sulfate filter were 14.8, 5.48 and 5.05 μGy per pulse, respectively, at 1.0 m, and the dimensions of the focal spot had values of 3.5×3.5 mm. Angiography was performed using both the aluminum and the barium sulfate filters at a charging voltage of 60 kV.

Keywords: energy-selective radiography, bremsstrahlung x rays, filtering, stroboscopic x-ray, pulse x-ray, angiography

1. INTRODUCTION

Modern high-speed x-ray generators are capable of producing short x-ray pulses with high dose rates, and have been applied to radiography in various fields. To produce hard flash x rays with maximum photon energies of approximately 1 MeV, multistage Marx surge generators have been developed.[1] Furthermore, induction linear accelerators[2] have been developed and improved to produce 10-MeV-order flash x rays. In contrast, 100-kV-order flash x-ray generators have been developed and applied to biomedicine.[3,4]

In the cases of multiple-shot and cine radiographies, we have developed several different repetitive-flash[5-8] and stroboscopic x-ray generators.[9-11] Although most flash x-ray generators have cold-cathode tubes, the stroboscopic generators utilize hot-cathode tubes. Particularly, although a 50 kHz stroboscopic generators have been manufactured, the repetition rate can be increased to MHz order.

Recently synchrotrons generate monochromatic parallel x-ray beams using a monochromator, and these beams have been employed to perform enhanced K-edge angiography[12,13] and x-ray phase imaging.[14,15] To perform angiography, the beams with photon energies of approximately 35 keV have been used, because iodine contrast mediums with a

26th International Congress on High-Speed Photography and Photonics, edited by D. L. Paisley, S. Kleinfelder, D. R. Snyder, B. J. Thompson, Proc. of SPIE Vol. 5580 (SPIE, Bellingham, WA, 2005) · 0277-786X/05/$15 · doi: 10.1117/12.568959

K-absorption edge of 33.155 keV absorb the beams effectively. In view of this situation, we have developed x-ray generators with cerium-target tubes[16,17] which can produce Kα rays of 34.6 keV.
In this research, we employed a tungsten-target x-ray tube and performed a preliminary study on high-speed angiography achieved with quasi-monochromatic x rays produced by filtering in conjunction with a computed radiography system.

2. GENERATOR

Figure 1 shows the block diagram of the kilohertz-range stroboscopic x-ray generator. This generator consists of the following major components: a main controller, a condenser unit with a Cockcroft-Walton circuit, and an x-ray tube unit in conjunction with a grid controller (Figs. 2 and 3). The main condenser of about 500 nF in the unit is charged up to 100 kV by the circuit, and the electric charges in the condenser are discharged to the triode by the grid control circuit. Although the tube voltage decreased during the discharging for generating x rays, the maximum value was equal to the initial charging voltage of the main condenser.
The x-ray tube is a glass-enclosed hot-cathode triode and is composed of the following major parts: an anode rod made of copper, a tungsten plate target, an iron focusing electrode, a tungsten hot cathode (filament), a tungsten grid, and a glass tube body. The electron beams from the cathode are accelerated between the anode and cathode electrodes and are converged to the target by the focusing electrode. The tube is set in the metal case filled with insulation oil, and the diaphragm regulates the radiation field.

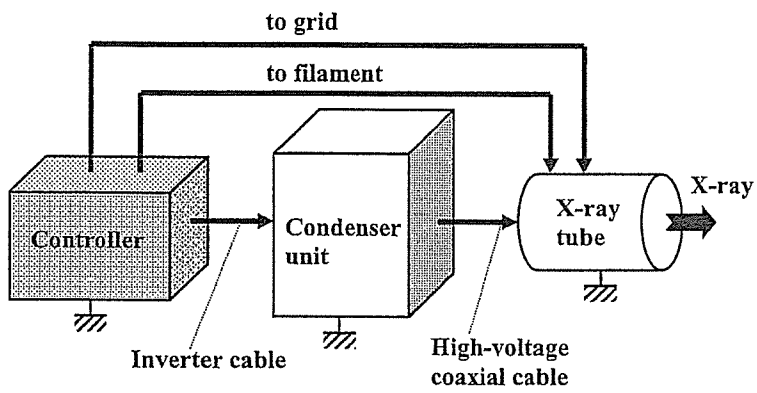

Figure 1: Block diagram of kilohertz-range stroboscopic x-ray generator.

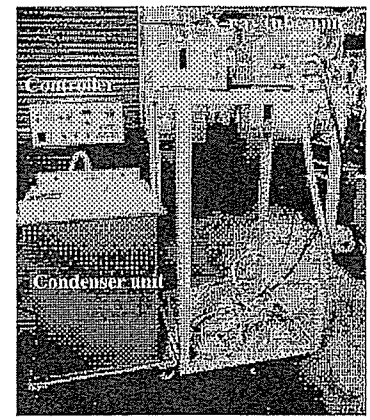

Figure 2: Stroboscopic x-ray generator.

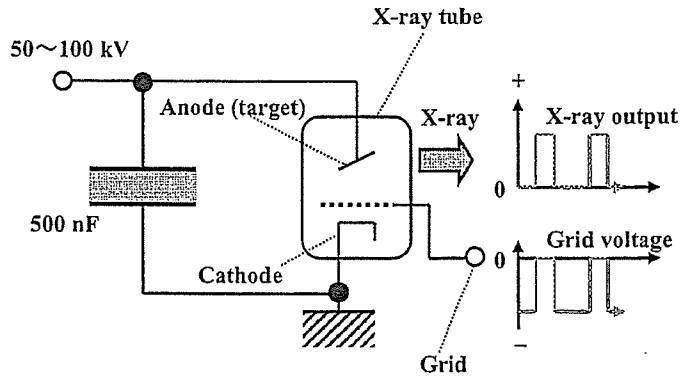

Figure 3: Main high-voltage circuit of x-ray generator.

3. CHARACTERISTICS

3.1 X-ray output

The x-ray output was detected by a pin diode, and the output voltages from the diode were measured by a digital storage scope (Fig. 4). Using this generator, the pulse width could be controlled correctly and ranged from 10 μs to 1.0 ms. The maximum repetition rate was approximately 50 kHz, and stable repetitive x-ray pulses were obtained. When the charging voltage was increased, the pulse height increased substantially.

3.2 Time-integrated x-ray intensity

Figure 5 shows the time-integrated (absolute) value of the x-ray intensity (exposure) at 1.0 m per pulse measured by a Victoreen 660 ionization chamber. The intensity was proportional to the driving pulse width. At a constant pulse width of 1.0 ms, the intensity increased in proportion to approximately the second power of the charging voltage. At a charging voltage of 80 kV and a width of 1.0 ms, the x-ray intensity obtained without filtering, using an aluminum filter, and using a barium sulfate filter were 14.8, 5.48, and 5.05 μGy per pulse, respectively, at 1.0 m from the source.

3.3 X-ray source

The image of the x-ray source was measured using a pinhole camera with a hole diameter of 50 μm and a computed radiography (CR) system (Konica Regius 150)[18] with a sampling pitch of 87.5 μm. When the charging voltage was increased, the dimensions hardly varied, and were approximately 3.5×3.5 mm.

3.4 X-ray spectra

In order to measure x-ray spectra, we employed a cadmium tellurium detector (CDTE2020X, Hamamatsu Photonics Inc.) (Fig. 6). Compared with a germanium detector, this detector has a lower energy resolution of 1.7 keV.
When the charging voltage was increased, both the maximum photon energy and the intensities of bremsstrahlung x rays increased, and the photon energy of the spectrum peak also increased. The 3-mm-thick aluminum filter attenuated the low-photon-energy bremsstrahlung x rays. Subsequently, the barium sulfate filter, with a surface density of approximately 10 mg/cm^2, significantly attenuated the spectra above the barium K-edge of 37.4 keV. The areas under the spectral curves correlate closely to the total x-ray intensities shown in Fig. 4.

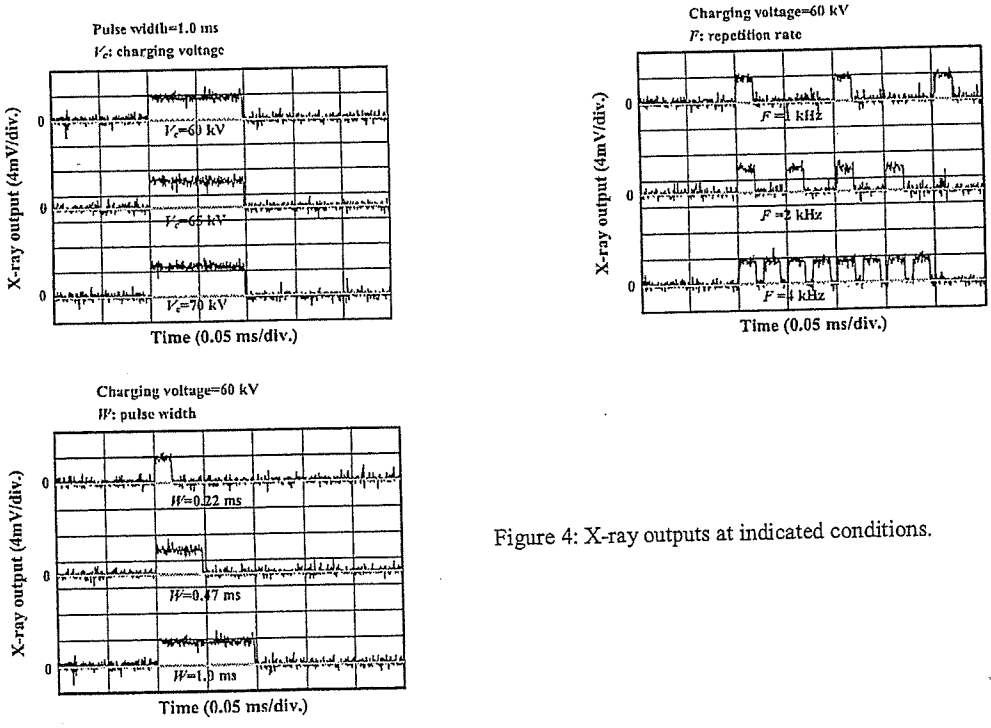

Figure 4: X-ray outputs at indicated conditions.

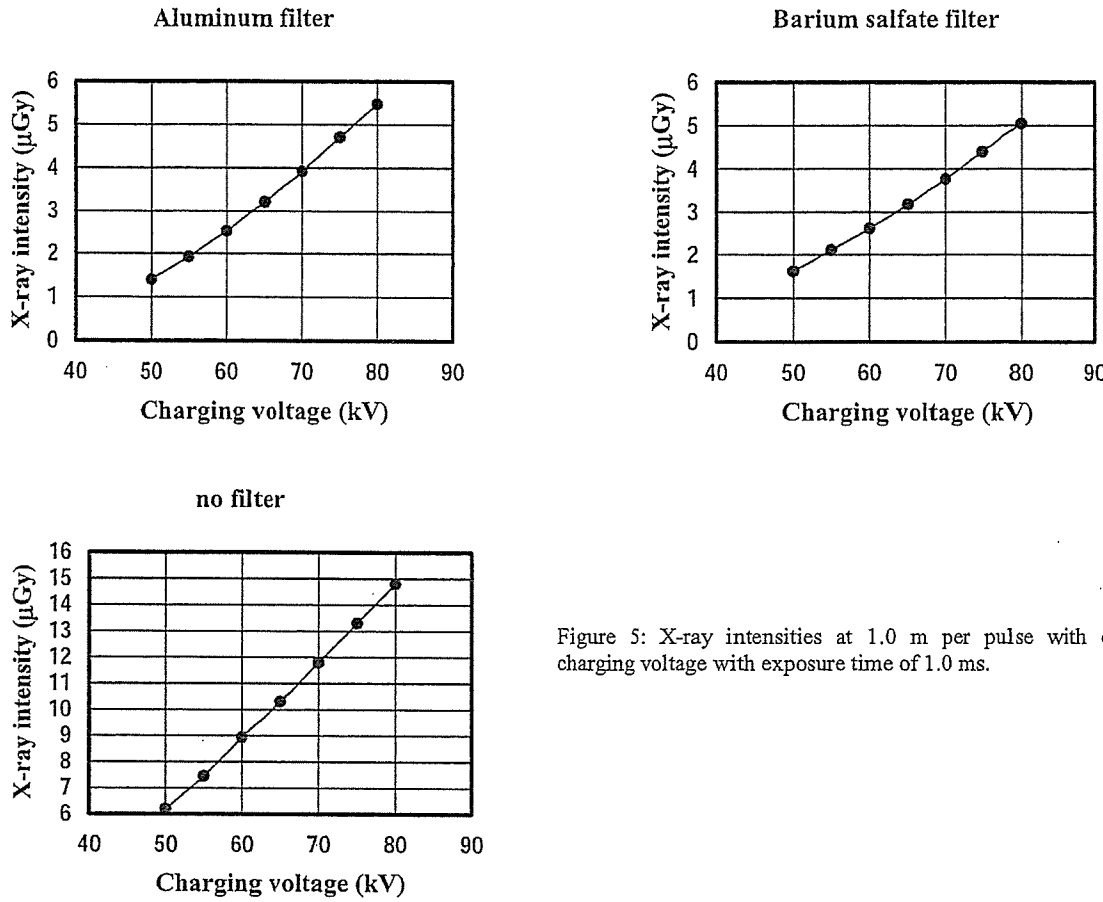

Figure 5: X-ray intensities at 1.0 m per pulse with changing charging voltage with exposure time of 1.0 ms.

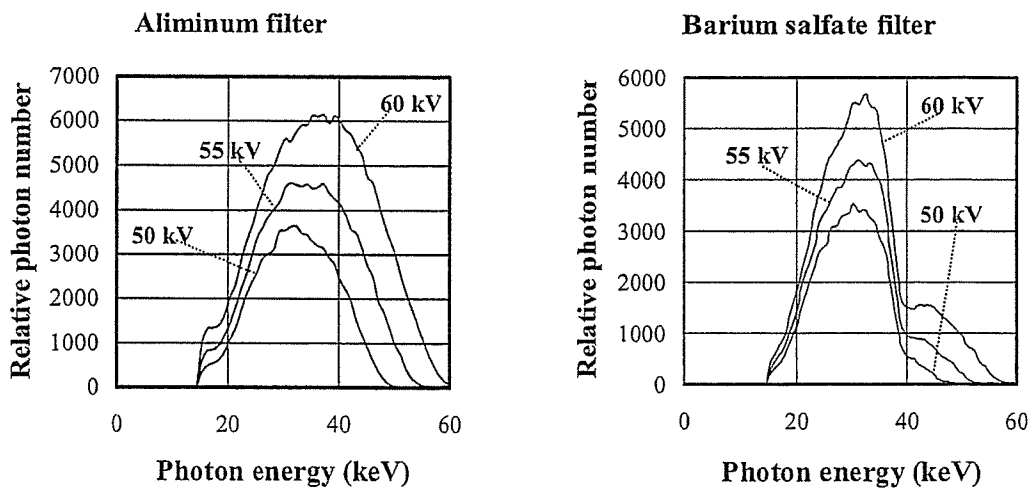

Figure 6: X-ray spectra at indicated conditions.

4. RADIOGRAPHY

The angiography was performed by a CR system using the filters with a charging voltage of 60 kV, and the distance between the x-ray source and the imaging plate was 0.7 m. The image contrast hardly varied even when the filter was changed.

Figure 7 shows radiograms of tungsten wires coiled around a rod made of polymethyl methacrylate using the aluminum filter. Although the image contrast increased with increases in the wire diameter, a 50 μm-diameter wire could be observed.

The image of water spouted from an injector is shown in Fig. 8. This image was taken with the slight addition of an iodine-based contrast medium using the barium sulfate filter. Because the x-ray duration was 1 ms, the stop-motion image of water could be obtained. Figures 9 and 10 show angiograms of a rabbit thigh (barium sulfate filter) and a dog heart (aluminum filter), respectively. In angiography, iodine-based microspheres of 15 μm in diameter were used, and fine blood vessels of about 100 μm were visible.

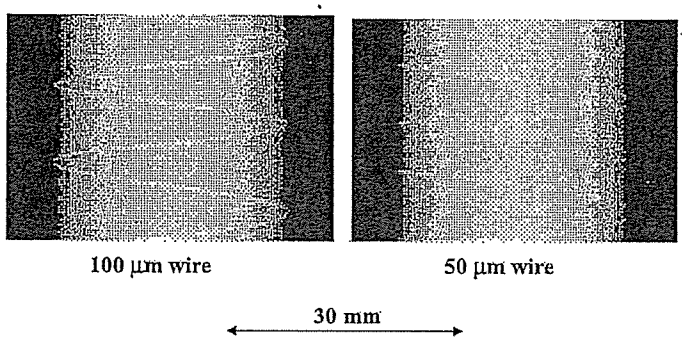

Figure 7: Radiograms of tungsten wires coiled around rod made of polymethyl methacrylate using aluminum filter.

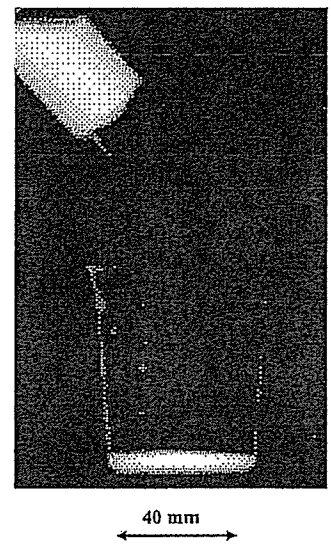

Figure 8: Radiogram of water spouted from injector using barium sulfate filter.

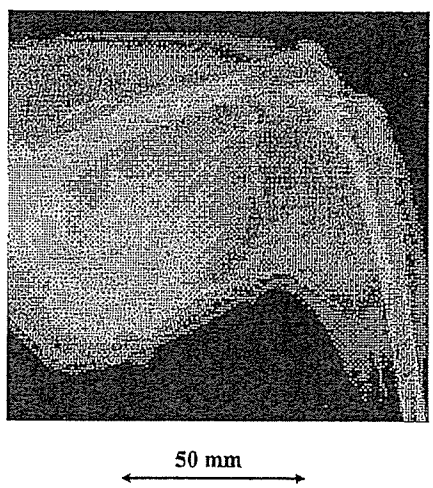

Figure 9: Angiograms of rabbit thigh achieved with barium sulfate filter.

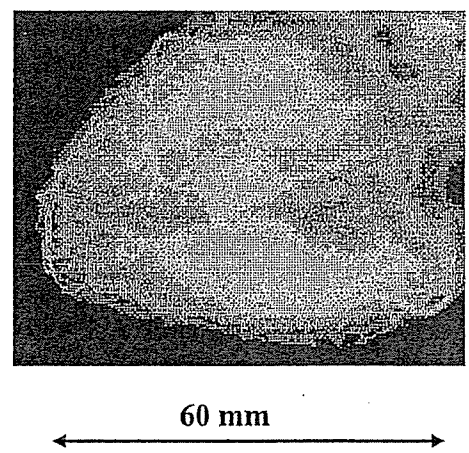

Figure 10: Angiogram of dog heart with aluminum filter.

5. DISCUSSION

Concerning the spectrum measurement, we obtained bremsstrahlung x rays with narrow energy latitudes using both the aluminum and the barium sulfate filters. When the aluminum filter was employed with a charging voltage of 60 kV, the peak photon energy of the spectra was approximately 35 kV. Therefore, the filter thickness should be increased in order to decrease bremsstrahlung x rays of lower than the K-absorption edge of iodine. Subsequently, using the barium sulfate filter, because the peak photon energy was nearly equal to the K-edge, aluminum filtering should be employed. In addition, a cerium oxide filter is also useful in order to increase the peak energy and to decrease low-photon-energy bremsstrahlung x rays.

Using these filters with a charging voltage of 60 kV and a pulse width (exposure time) of 1.0 ms, although we obtained the x-ray intensities of approximately 5 μGy at 1.0 m per pulse, the intensity should be maximized by increasing the tube current in order to improve the image quality using the CR system.

With recent advances in angiography using MRI, if the density of gadolinium-based contrast mediums increases, enhanced K-edge angiography utilizing monochromatic x-ray generators, which produce tungsten Kα rays, will be a useful technique to decrease the absorbed dose during angiography.

ACKNOWLEDGMENT

This work was supported by Grants-in-Aid for Scientific Research (13470154, 13877114, and 16591222) and Advanced Medical Scientific Research from MECSST, Health and Labor Sciences Research Grants(RAMT-nano-001, RHGTEFB-genome-005 and RHGTEFB-saisei-003), Grants from Keiryo Research Foundation, The Promotion and Mutual Aid Corporation for Private Schools of Japan, Japan Science and Technology Agency (JST), and New Energy and Industrial Technology Development Organization (NEDO, Industrial Technology Research Grant Program in '03).

REFERENCES

1. R. Germer, "X-ray flash techniques," *J. Phys. E: Sci. Instrum.*, **12**, 336-350, 1979.
2. C. Cavailler, "AIRIX- a new tool for flash radiography in detonics," *SPIE*, **4183**, 23-35, 2000.
3. E. Sato, M. Sagae, A. Shikoda, K. Takahashi, T. Oizumi, M. Yamamoto, A. Takabe, K. Sakamaki, Y. Hayasi, H. Ojima, K. Takayama and Y. Tamakawa, "High-speed soft x-ray techniques," *SPIE*, **2869**, 937-955, 1996.
4. E. Sato, M. Sagae, E. Tanaka, Y. Hayasi, R. Germer, H. Mori, T. Kawai, T. Ichimaru, S. Sato, K. Takayama and H. Ido: Quasi-monochromatic flash x-ray generator utilizing a disk-cathode molybdenum tube, *Jpn. J. Appl. Phys.*, **43**, 7324-7328, 2004.
5. E. Sato, S. Kimura, S. Kawasaki, H. Isobe, K. Takahashi, Y. Tamakawa and T. Yanagisawa, "Repetitive flash x-ray generator utilizing a simple diode with a new type of energy-selective function," *Rev. Sci. Instrum.*, **61**, 2343-2348, 1990.
6. A. Shikoda, E. Sato, M. Sagae, T. Oizumi, Y. Tamakawa and T. Yanagisawa, "Repetitive flash x-ray generator having a high-durability diode driven by a two-cable-type line pulser," *Rev. Sci. Instrum.*, **65**, 850-856, 1994.
7. E. Sato, K. Takahashi, M. Sagae, S. Kimura, T. Oizumi, Y. Hayasi, Y. Tamakawa and T. Yanagisawa, "Sub-kilohertz flash x-ray generator utilizing a glass-enclosed cold-cathode triode," *Med. & Biol. Eng. & Comput.*, **32**, 289-294, 1994.
8. K. Takahashi, E. Sato, M. Sagae, T. Oizumi, Y. Tamakawa and T. Yanagisawa, "Fundamental study on a long-duration flash x-ray generator with a surface-discharge triode," *Jpn. J. Appl. Phys.*, **33**, 4146-4151, 1994.
9. E. Sato, M. Sagae, K. Takahashi, A. Shikoda, T. Oizumi, Y. Hayasi, Y. Tamakawa and T. Yanagisawa, "10 kHz microsecond pulsed x-ray generator utilizing a hot-cathode triode with variable durations for biomedical radiography," *Med. & Biol. Eng. & Comput.*, **32**, 295-301, 1994.
10. E. Sato, T. Ichimaru, H. Obara, M. Zuguchi, H. Mori, E. Tanaka, T. Usuki, K. Sato, H. Ojima, K. Takayama, K. Sakamaki and Y. Tamakawa, "Condenser-discharge stroboscopic x-ray generator for medical radiography," *SPIE*, **4183**, p383-393, 2000.
11. E. Sato, H. Ojima, K. Takayama, M. Matsumasa, H. Obara, M. Zuguchi, T. Usuki, K. Sato, K. Sakamaki and Y. Tamakawa, "Observation of cavitation bubble cloud using a stroboscopic x-ray generator," *SPIE*, **4183**, 394-404, 2000.
12. H. Mori, K. Hyodo, E. Tanaka, M. U. Mohammed, A. Yamakawa, Y. Shinozaki, H. Nakazawa, Y. Tanaka, T. Sekka, Y. Iwata, S. Honda, K. Umetani, H. Ueki, T. Yokoyama, K. Tanioka, M. Kubota, H. Hosaka, N. Ishizawa and M. Ando, "Small-vessel radiography in situ with monochromatic synchrotoron radiation," *Radiology*, **201**, 173-177, 1996.

13. K. Hyodo, M. Ando, Y. Oku, S. Yamamoto, T. Takeda, Y. Itai, S. Ohtsuka, Y. Sugishita and J. Tada, "Development of a two-dimensional imaging system for clinical applications of intravenous coronary angiography using intense synchrotron radiation produced by a multipole wiggler," *J. Synchrotron Rad.*, **5**, 1123-1126, 1998.
14. A. Momose, T. Takeda, Y. Itai and K. Hirano, "Phase-contrast x-ray computed tomography for observing biological soft tissues," *Nature Medicine*, **2**, 473-475, 1996.
15. M. Ando, A. Maksimenko, H. Sugiyama, W. Pattanasiriwisawa, K. Hyodo and C. Uyama, "A simple x-ray dark- and bright- field imaging using achromatic Laue optics, *Jpn. J. Appl. Phys.*, **41**, L1016-L1018, 2002.
16. E. Sato, R. Germer, Y. Hayasi, K. Murakami, Y. Koorikawa, E. Tanaka, H. Mori, T. Kawai, T. Ichimaru, F. Obata, K. Takahashi, S. Sato, K. Takayama and Ido, H.: Weakly ionized cerium plasma radiography, *SPIE*, **5210**, 12-21, 2003.
17. E. Sato, E. Tanaka, H. Mori, T. Kawai, T. Ichimaru, S. Sato, K. Takayama and H. Ido, "Demonstration of enhanced K-edge angiography using a cerium target x-ray generator," *Med. Phys,* **31**, 3017-3021, 2004.
18. E. Sato, K. Sato and Y. Tamakawa, "Film-less computed radiography system for high-speed imaging," *Ann. Rep. Iwate Med. Univ. Sch. Lib. Arts and Sci.*, **35**, 13-23, 2000.
*dresato@iwate-med.ac.jp; phone, phone +81-19-651-5111; fax +81-19-654-9282

High-speed enhanced K-edge angiography utilizing cerium plasma x-ray generator

Eiichi Sato, MEMBER SPIE
Iwate Medical University
Department of Physics
Morioka 020-0015, Japan
E-mail: dresato@iwate-med.ac.jp

Etsuro Tanaka
Tokyo University of Agriculture
Department of Nutritional Science
Faculty of Applied Bioscience
Setagaya-ku 156-8502, Japan

Hidezo Mori
National Cardiovascular Center Research Institute
Department of Cardiac Physiology
Osaka 565-8565, Japan

Toshiaki Kawai, MEMBER SPIE
Hamamatsu Photonics K. K.
Electron Tube Division #2
Iwata-gun 438-0193, Japan

Shigehiro Sato
Iwate Medical University
Department of Microbiology
School of Medicine
Morioka 020-8505, Japan

Kazuyoshi Takayama, MEMBER SPIE
Tohoku University
Shock Wave Research Center
Institute of Fluid Science
Sendai 980-8577, Japan

Abstract. The cerium target plasma flash x-ray generator is useful to perform high-speed enhanced K-edge angiography using cone beams, because K-series characteristic x-rays from the cerium target are absorbed effectively by iodine-based contrast mediums. In the plasma generator, a 200-nF condenser is charged up to 60 kV by a power supply, and flash x-rays are produced by the discharging. The x-ray tube is a demountable triode with a trigger electrode, and the turbomolecular pump evacuates air from the tube with a pressure of approximately 1 mPa. Target evaporation leads to the formation of weakly ionized linear plasma, consisting of cerium ions and electrons, around the target, and intense flash x-rays are produced. At a charging voltage of 55 kV, the maximum tube voltage is almost equal to the charging voltage of the main condenser, and the maximum current is approximately 20 kA. When the charging voltage is increased, weakly ionized cerium plasma forms, and the K-series characteristic x-ray intensities increase. The x-ray pulse widths are about 500 ns, and the time-integrated x-ray intensity has a value of about 40 μC/kg at 1.0 m from the x-ray source with a charging voltage of 55 kV. In the angiography, we employ a filmless computed radiography (CR) system and iodine-based microspheres.

[DOI: 10.1117/1.1882372]

Subject terms: plasma x-ray; cerium target; weakly ionized cerium plasma; characteristic x-ray; K-edge angiography.

Paper 040183 received Mar. 26, 2004; revised manuscript received Sep. 9, 2004; accepted for publication Oct. 25, 2004; published online Apr. 6, 2005. This paper is a revision of a paper presented at the SPIE conference on Ultrahigh- and High-Speed Photography, Photonics, and Videography, Aug. 2003, San Diego, California. The paper presented there appears (unrefereed) in SPIE Proceedings Vol. 5210.

1 Introduction

Flash x-rays are useful to perform high-speed radiography, and various generators have been developed to correspond to specific radiographic objectives.[1–5] In the cases of multishot and cine radiographies, we have developed several different repetitive-flash[6–10] and stroboscopic x-ray generators.[11–17] Although most flash x-ray generators have cold-cathode tubes, the stroboscopic generators utilize hot-cathode tubes.

In conjunction with single crystals, synchrotrons generate monochromatic x-rays. These rays play important roles in parallel radiography and have been employed to perform high-contrast K-edge angiography[18] and x-ray phase imaging.[19,20] However, it is difficult to obtain sufficient machine times for various research projects, including medical applications.

As for angiography using iodine-based contrast mediums, K-series characteristic x-rays of cerium are extremely useful, since the rays are absorbed easily by iodine. In particular, since fairly intense and sharp characteristic x-rays have been produced from weakly ionized linear plasmas[21–24] of nickel, copper, and molybdenum, the development of a cerium-target x-ray tube for angiography is highly desirable.

In this research, we developed a single flash x-ray generator with a cerium-target plasma tube and performed a preliminary study on weakly ionized cerium plasma angiography.

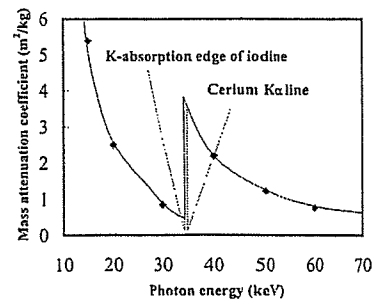

Fig. 1 Relation between mass attenuation coefficient of iodine and average photon energy of cerium Kα lines.

0091-3286/2005/$22.00 © 2005 SPIE

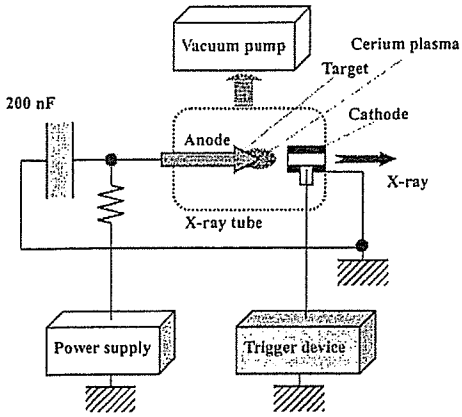

Fig. 2 Block diagram of high intensity plasma flash x-ray generator.

2 Principle of K-Edge Angiography

Figure 1 shows the mass attenuation coefficients of iodine at the selected energies; the coefficient curve is discontinuous at the iodine K-edge. The average photon energy of the cerium Kα lines is shown just above the iodine K-edge. Cerium is a rare earth element and has a high reactivity; however, the average photon energy of Kα lines is 34.566 keV, and iodine contrast mediums with a K-absorption edge of 33.155 keV absorb the lines easily. Therefore, blood vessels were observed with high contrasts.

3 Generator

3.1 *High-Voltage Circuit*

Figure 2 shows a block diagram of a high-intensity plasma flash x-ray generator. This generator consists of the following essential components: a high-voltage power supply, a high-voltage condenser with a capacity of about 200 nF, a turbomolecular pump, a krytron pulse generator as a trigger device, and a flash x-ray tube. The high-voltage main condenser is charged up to 60 kV by the power supply, and

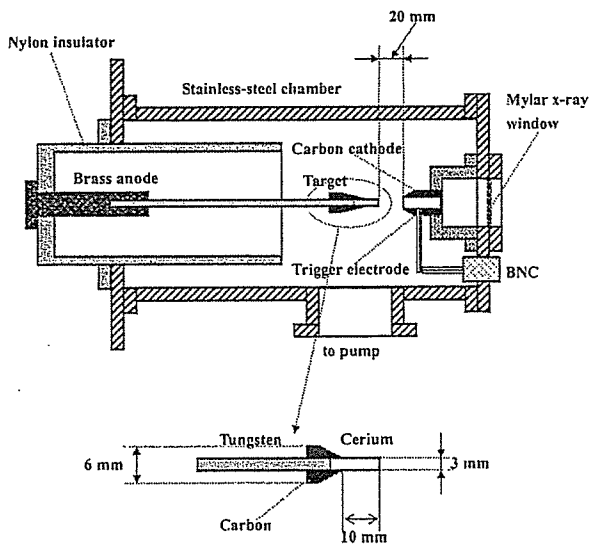

Fig. 3 Schematic drawing of flash x-ray tube.

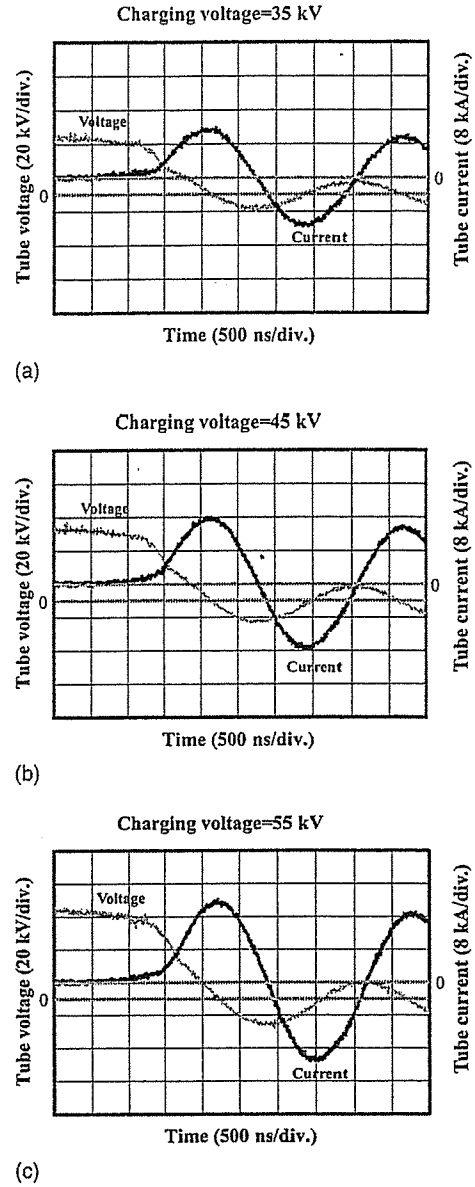

Fig. 4 Tube voltages and currents with charging voltage of (a) 35, (b) 45, and (c) 55 kV.

electric charges in the condenser are discharged to the tube after triggering the cathode electrode by the trigger device. The plasma flash x-rays are then produced.

3.2 *X-Ray Tube*

The x-ray tube is a demountable cold-cathode triode that is connected to the turbomolecular pump with a pressure of approximately 1 mPa (Fig. 3). This tube consists of the following major parts: a hollow cylindrical carbon cathode with a bore diameter of 10.0 mm, a trigger electrode made from a copper wire, a stainless-steel vacuum chamber, a nylon insulator, a polyethylene terephthalate (Mylar) x-ray window of 0.25 mm, and a rod-shaped cerium target of 3.0 mm in diameter. The target tip is embedded in the carbon rod to absorb the characteristic x-rays of carbon by the window. The distance between the target and cathode electrodes is approximately 20 mm, and the trigger electrode is

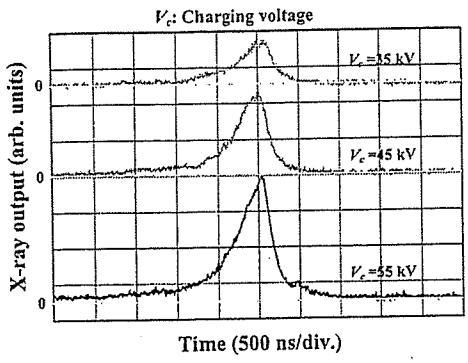

Fig. 5 X-ray outputs at indicated conditions.

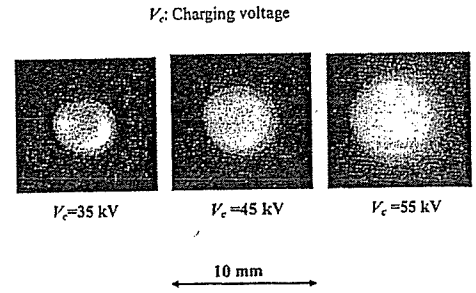

Fig. 6 Images of plasma x-ray source.

set in the cathode electrode. As electron beams from the cathode electrode are roughly converged to the target by an electric field in the tube, the weakly ionized plasma, which consists of cerium ions and electrons, forms around the target by evaporating.

4 Characteristics

4.1 *Tube Voltage and Current*

Tube voltage and current were measured by a high-voltage divider with an input impedance of 1 GΩ and a current transformer, respectively. Figure 4 shows the time relation between the tube voltage and current. At the indicated charging voltages, they roughly displayed damped oscillations. When the charging voltage was increased, both the maximum tube voltage and current increased. At a charging voltage of 55 kV, the maximum tube voltage was almost equal to the charging voltage of the main condenser, and the maximum tube current was about 20 kA.

4.2 *X-Ray Output*

An x-ray output pulse was detected using a combination of a plastic scintillator and a photomultiplier. The x-ray pulse height substantially increased with corresponding increases in the charging voltage (Fig. 5). The x-ray pulse widths were about 500 ns, and the time-integrated x-ray intensity measured by a thermoluminescence dosimeter (Kyokko TLD Reader 1500 utilizing MSO-S elements without energy compensation) had a value of about 40 μC/kg at 1.0 m from the x-ray source with a charging voltage of 55 kV.

4.3 *X-Ray Source*

To measure images of the plasma x-ray source, we employed a pinhole camera with a hole diameter of 100 μm (Fig. 6). When the charging voltage was increased, the plasma x-ray source grew, and both spot dimension and intensity increased. Because the x-ray intensity is the highest at the center of the spot, both the dimension and intensity decreased according to both increases in the thickness of a filter for absorbing x-rays and decreases in the pinhole diameter.

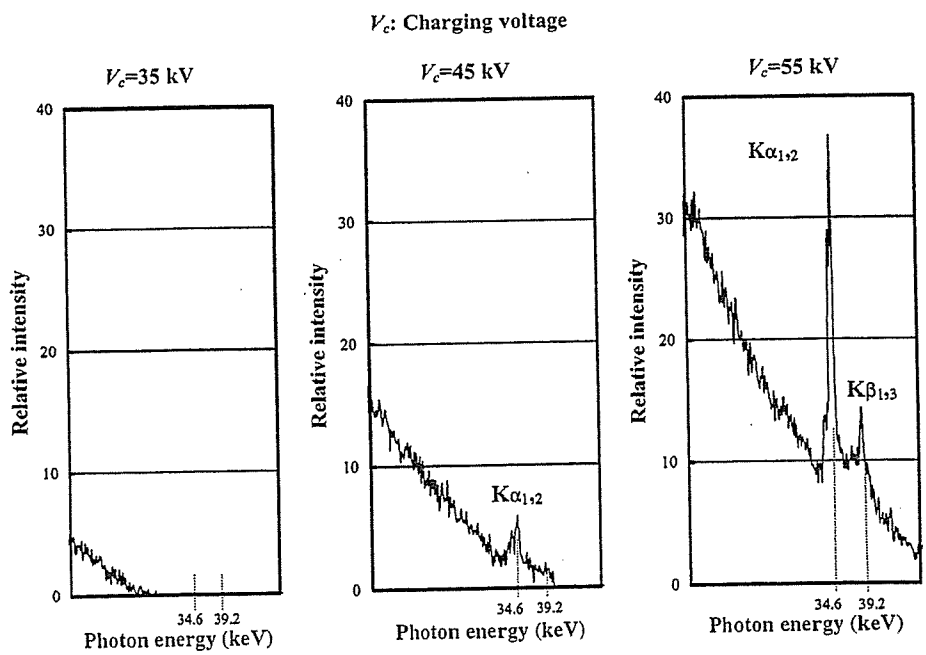

Fig. 7 X-ray spectra from weakly ionized cerium plasma.

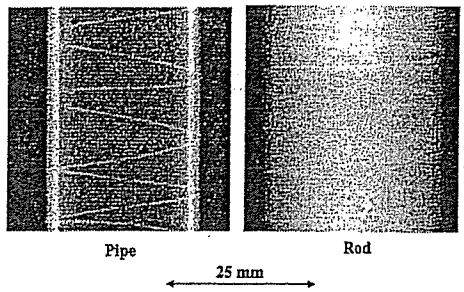

Fig. 8 Radiograms of tungsten wires of 50 μm in diameter coiled around pipe and rod made of PMMA.

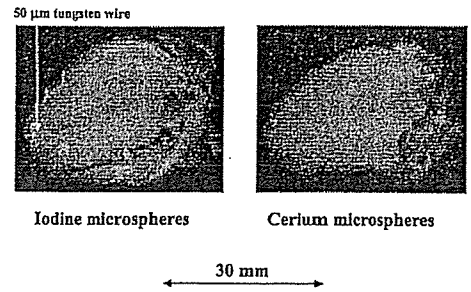

Fig. 10 Angiograms of rabbit hearts using iodine and cerium microspheres.

4.4 *X-Ray Spectra*

X-ray spectra from the plasma source were measured by a transmission-type spectrometer with a lithium fluoride curved crystal of 0.5 mm in thickness. The spectra were taken by a computed radiography (CR) system[25] (Konica Regius 150) having a wide dynamic range, and relative x-ray intensity was calculated from Dicom digital data. Figure 7 shows measured spectra from the cerium target. In this experiment, although we observed both the bremsstrahlung and characteristic x-rays, we could not observe characteristic x-rays with a charging voltage of 35 kV, because the critical excitation energy is 40.3 keV. Both intensities increased substantially with increases in the charging voltage.

5 Angiography

The plasma angiography was performed by the CR system without using a monochromatic filter, and the distance between the x-ray source and the imaging plate was 1.2 m.

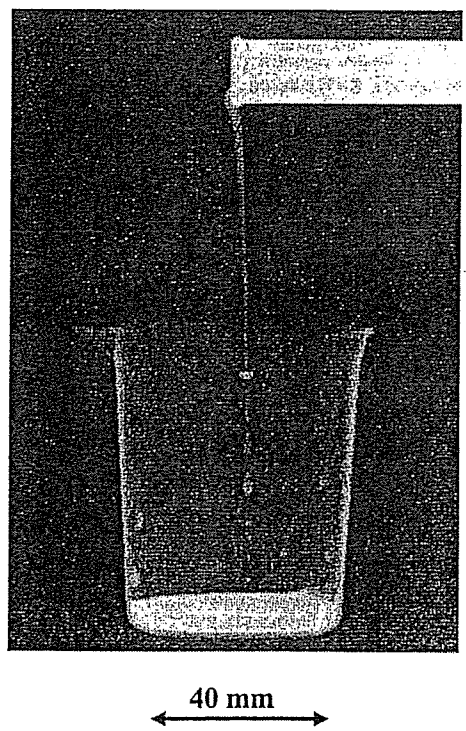

Fig. 9 Radiogram of water falling into a polypropylene beaker from a glass test tube.

Subsequently, in angiography testing, we usually employ nonliving animal phantoms using microspheres.

First, rough measurements of image resolution were made using wires. Figure 8 shows radiograms of 50-μm-diam tungsten wires coiled around a pipe, and a rod made of polymethyl methacrylate (PMMA) with a charging voltage of 55 kV. Although the image contrast increased using the pipe, 50-μm-diam wires could be observed.

The image of water falling into a polypropylene beaker from a glass test tube is shown in Fig. 9. This image was taken with a charging voltage of 55 kV, with the slight addition of an iodine-based contrast medium. Because the x-ray duration was about 1 μs, the stop-motion image of water could be obtained.

Angiograms of rabbit hearts are shown in Fig. 10. These two images were obtained using iodine and cerium microspheres of 15 μm, respectively, with a charging voltage of 55 kV. In cases where the cerium spheres were employed, the coronary arteries were barely visible. Figure 11 shows an angiogram of the external ear of a rabbit using iodine spheres with a charging voltage of 55 kV, and fine blood vessels of about 50 μm are visible. In angiography of a larger heart extracted from a dog, using iodine spheres, a PMMA plate was set in front of a heart facing x-ray source, and image contrast of coronary arteries improved with increases in the plate thickness (Fig. 12).

6 Discussion

In an earlier experiment using a copper target,[24] bremsstrahlung x-rays were hardly observed at all, and we confirmed the irradiation of fairly clean K-series characteristic x-rays such as lasers. In the present work, although we confirmed intense characteristic x-rays with a higher charging voltage, bremsstrahlung x-rays were detected, since the bremsstrahlung intensity is proportional to the atomic num-

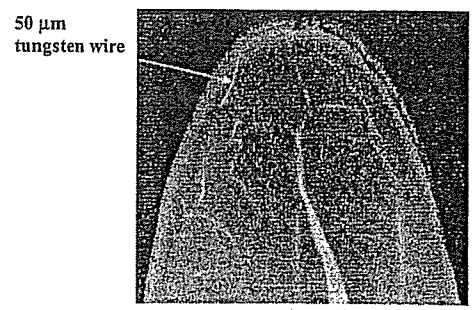

Fig. 11 Angiograms of external ear of rabbit.

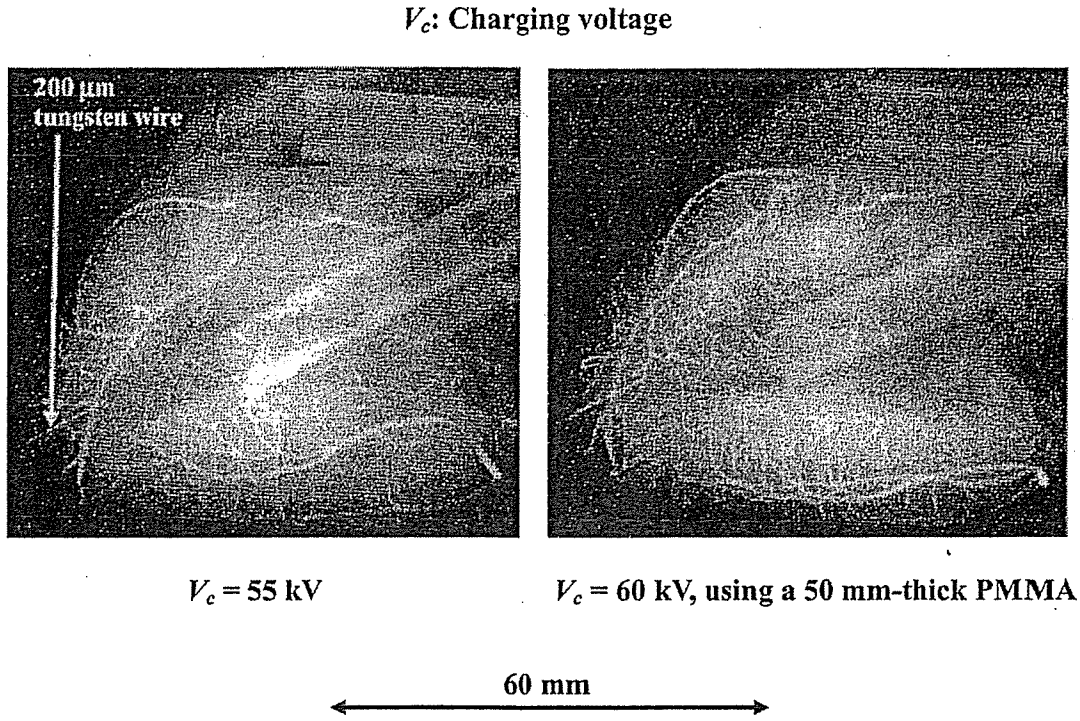

Fig. 12 Angiograms of extracted heart of dog.

ber of the target element, and high-photon-energy bremsstrahlung x-rays are not absorbed effectively in the plasma. Therefore, the condenser charging voltage should be raised as high as possible to increase the characteristic x-ray intensity. To decrease emission of bremsstrahlung x-rays from the carbon target holder, the target length should also be set as long as possible. Next, since the spheres easily transmit bremsstrahlung x-rays with energies lower than the edge, it is important that the rays be absorbed as much as possible before angiography to increase the image contrast.

In this research, we obtained sufficient x-ray intensity per pulse for CR radiography, and the generator produced high-dose-rate plasma x-rays of approximately 80 C/kg·s at 1.0 m with a charging voltage of 55 kV. In addition, because the x-ray intensity increases with increases in the electrostatic energy in the main discharge condenser, the flash x-rays from weakly ionized linear cerium plasma can be employed to perform high-speed angiography for cardiovascular disease.

Acknowledgments

This work was supported by Grants-in-Aid for Scientific Research (13470154, 13877114, and 16591222) and Advanced Medical Scientific Research from MECSST; Health and Labor Sciences Research Grants (RAMT-nano-001, RHGTEFB-genome-005, and RHGTEFB-saisei-003); and grants from Keiryo Research Foundation, The Promotion and Mutual Aid Corporation for Private Schools of Japan, Japan Science and Technology Agency (JST), and New Energy and Industrial Technology Development Organization (NEDO, Industrial Technology Research Grant Program in '03).

References

1. A. Mattsson, "Some characteristics of a 600 kV flash x-ray tube," *Phys. Scr.* **5**, 99–102 (1972).
2. R. Germer, "X-ray flash techniques," *J. Phys. E* **12**, 336–350 (1979).
3. E. Sato, H. Isobe, and F. Hoshino, "High intensity flash x-ray apparatus for biomedical radiography," *Rev. Sci. Instrum.* **57**, 1399–1408 (1986).
4. E. Sato, M. Sagae, K. Takahashi, T. Oizumi, H. Ojima, K. Takayama, Y. Tamakawa, T. Yanagisawa, A. Fujiwara, and K. Mitoya, "High-speed soft x-ray generators in biomedicine," *Proc. SPIE* **2513**, 649–667 (1994).
5. E. Sato, M. Sagae, A. Shikoda, K. Takahashi, T. Oizumi, M. Yamamoto, A. Takabe, K. Sakamaki, Y. Hayasi, H. Ojima, K. Takayama, and Y. Tamakawa, "High-speed soft x-ray techniques," *Proc. SPIE* **2869**, 937–955 (1996).
6. E. Sato, S. Kimura, S. Kawasaki, H. Isobe, K. Takahashi, Y. Tamakawa, and T. Yanagisawa, "Repetitive flash x-ray generator utilizing a simple diode with a new type of energy-selective function," *Rev. Sci. Instrum.* **61**, 2343–2348 (1990).
7. S. Kimura, E. Sato, M. Sagae, A. Shikoda, T. Oizumi, K. Takahashi, Y. Tamakawa, and T. Yanagisawa, "Disk-cathode flash x-ray tube driven by a repetitive two-stage Marx pulser," *Med. Biol. Eng. Comput.* **31**, S37–S43 (1993).
8. A. Shikoda, E. Sato, M. Sagae, T. Oizumi, Y. Tamakawa, and T. Yanagisawa, "Repetitive flash x-ray generator having a high-durability diode driven by a two-cable-type line pulser," *Rev. Sci. Instrum.* **65**, 850–856 (1994).
9. E. Sato, K. Takahashi, M. Sagae, S. Kimura, T. Oizumi, Y. Hayasi, Y. Tamakawa, and T. Yanagisawa, "Sub-kilohertz flash x-ray generator utilizing a glass-enclosed cold-cathode triode," *Med. Biol. Eng. Comput.* **32**, 289–294 (1994).
10. K. Takahashi, E. Sato, M. Sagae, T. Oizumi, Y. Tamakawa, and T. Yanagisawa, "Fundamental study on a long-duration flash x-ray generator with a surface-discharge triode," *Jpn. J. Appl. Phys.* **33**, 4146–4151 (1994).
11. E. Sato, A. Shikoda, S. Kimura, M. Sagae, H. Isobe, Y. Tamakawa, and T. Yanagisawa, "Kilohertz-range flash x-ray generator utilizing a triode in conjunction with an extremely hot cathode," *Rev. Sci. Instrum.* **62**, 2115–2120 (1991).
12. E. Sato, M. Sagae, K. Takahashi, A. Shikoda, T. Oizumi, Y. Hayasi, Y. Tamakawa, and T. Yanagisawa, "10 kHz microsecond pulsed x-ray generator utilizing a hot-cathode triode with variable durations for biomedical radiography," *Med. Biol. Eng. Comput.* **32**, 295–301 (1994).
13. E. Sato, T. Ichimaru, T. Usuki, K. Sato, H. Ojima, K. Takayama, H.

Ido, K. Sakamaki, and Y. Tamakawa, "Condenser-discharge stroboscopic x-ray generator SX-C98," *Proc. SPIE* **3516**, 618–625 (1998).
14. E. Sato, T. Ichimaru, H. Ojima, K. Takayama, H. Ido, and Y. Tamakawa, "Characteristics of the kilohertz-range harder stroboscopic x-ray generator and applications," *Proc. SPIE* **3771**, 12–21 (1999).
15. E. Sato, T. Ichimaru, H. Obara, M. Zuguchi, H. Mori, E. Tanaka, T. Usuki, K. Sato, H. Ojima, K. Takayama, K. Sakamaki, and Y. Tamakawa, "Condenser-discharge stroboscopic x-ray generator for medical radiography," *Proc. SPIE* **4183**, 383–393 (2000).
16. E. Sato, H. Ojima, K. Takayama, M. Matsumasa, H. Obara, M. Zuguchi, T. Usuki, K. Sato, K. Sakamaki, and Y. Tamakawa, "Observation of cavitation bubble cloud using a stroboscopic x-ray generator," *Proc. SPIE* **4183**, 394–404 (2000).
17. E. Sato, Y. Hayasi, and Y. Tamakawa, "Recent stroboscopic x-ray generators and their applications to high-speed radiography," *Ann. Rep. Iwate Med. Univ. Lib. Arts and Sci.* **35**, 1–11 (2000).
18. H. Mori, K. Hyodo, E. Tanaka, M. U. Mohammed, A. Yamakawa, Y. Shinozaki, H. Nakazawa, Y. Tanaka, T. Sekka, Y. Iwata, S. Honda, K. Umetani, H. Ueki, T. Yokoyama, K. Tanioka, M. Kubota, H. Hosaka, N. Ishizawa, and M. Ando, "Small-vessel radiography in situ with monochromatic synchrotoron radiation," *Radiology* **201**, 173–177 (1996).
19. T. J. Davis, D. Gao, T. E. Gureyev, A. W. Stevenson, and S. W. Wilkims, "Phase-contrast imaging of weakly absorbing materials using hard x-rays," *Nature (London)* **373**, 595–597 (1995).
20. A. Momose, T. Takeda, Y. Itai, and K. Hirano, "Phase-contrast x-ray computed tomography for observing biological soft tissues," *Nat. Med.* **2**, 473–475 (1996).
21. E. Sato, Y. Hayasi, E. Tanaka, H. Mori, T. Kawai, T. Usuki, K. Sato, H. Obara, T. Ichimaru, K. Takayama, H. Ido, and Y. Tamakawa, "Quasi-monochromatic radiography using a high-intensity quasi-x-ray laser generator," *Proc. SPIE* **4682**, 538–548 (2002).
22. E. Sato, Y. Hayasi, R. Germer, E. Tanaka, H. Mori, T. Kawai, H. Obara, T. Ichimaru, K. Takayama, and H. Ido, "Intense characteristic x-ray irradiation from weakly ionized linear plasma and applications," *Jpn. J. Med. Imag. Inform. Sci.* **20**, 148–155 (2003).
23. E. Sato, Y. Hayasi, R. Germer, E. Tanaka, H. Mori, T. Kawai, H. Obara, T. Ichimaru, K. Takayama, and H. Ido, "Irradiation of intense characteristic x-rays from weakly ionized linear molybdenum plasma," *Jpn. J. Med. Phys.* **23**, 123–131 (2003).
24. E. Sato, Y. Hayasi, R. Germer, E. Tanaka, H. Mori, T. Kawai, T. Ichimaru, K. Takayama, and Hideaki Ido, "Quasi-monochromatic flash x-ray generator utilizing weakly ionized linear copper plasma," *Rev. Sci. Instrum.* **74**, 5236–5240 (2003).
25. E. Sato, K. Sato, and Y. Tamakawa, "Film-less computed radiography system for high-speed Imaging," *Ann. Rep. Iwate Med. Univ. Sch. Lib. Arts Sci.* **35**, 13–23 (2000).

Eiichi Sato received his BS, MS, and PhD in applied physics from Tohoku Gakuin University, Sendai, Japan, in 1979, 1982, and 1987, respectively. From 1982, he was an assistant in the Department of Physics, and became an associate professor in 1986. Since 2004, he has been a professor of physics at Iwate Medical University. He has written some 400 publications and delivered some 200 international presentations concerning x-rays. His research interests include soft flash x-ray generators, quasi-x-ray laser generators, and high-speed radiography. In 2000 he received the Schardin Gold Medal from the German Physical Society, and in 2003 he received the Takayama Award (Gold Medal) from the Japan Society of High Speed Photography and Photonics.

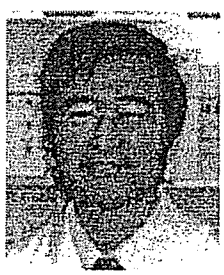

Etsuro Tanaka received his MD and PhD degrees in medicine from Kumamoto University, Japan, in 1980 and 1986, respectively. He worked on medical image processing in the Department of Physiology, Tokai University, Japan, from 1988 to 2003. He is currently a professor in the Department of Nutritional Sciences, Tokyo University of Agriculture, Japan. His research interests include medical image processing, human physiology, and clinical nutrition.

Hidezo Mori received a medical degree from Keio University School of Medicine, Tokyo, Japan, in 1977, and also a PhD from the Post Graduate School, Keio University School of Medicine. Now he is the director of the Department of Cardiac Physiology at the National Cardiovascular Center, Suita, Japan. His primary research interests are regenerative therapy in cardiovascular disease, microcirculation, and medical applications of structural biology.

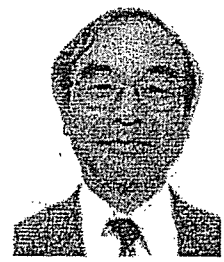

Toshiaki Kawai received the BS degree in precision mechanics and the MS degree in electronic engineering from Shizuoka University, Hamamatsu, Japan, in 1964 and 1974, respectively. In 1974, he joined the Hamamatsu Photonics K.K., where he worked on research and development of solid-state infrared detectors, and then from 1978 to 1981 engaged in research work on the NEA cold cathode for application to imaging camera tubes. He is now the project coordinator of the Electron Tube Division #2 and is engaged in the development and manufacturing of imaging devices and x-ray equipment. He is a member of the Japan Radioisotope Association and the Institute of Image Information and Television Engineers of Japan.

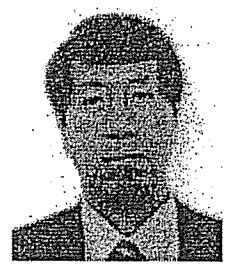

Shigehiro Sato received his MD degree from Iwate Medical University in 1980. He worked for the laboratory of the Division of Pediatric Infectious Diseases at Johns Hopkins Hospital from 1985 to 1989. He is currently a professor in the Department of Microbiology at Iwate Medical University. His research interests include central nervous system damage caused by Vero toxin, a cell culture system for vaccine development, and microangiography.

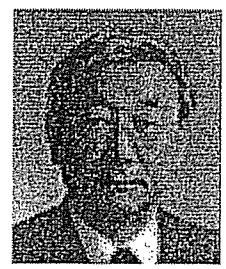

Kazuyoshi Takayama received his BS degree from Nagoya Institute of Technology in 1962. In 1970, he received his PhD in mechanical engineering from Tohoku University. Since 1986, he has been a director (professor) of the Shock Wave Research Center, Institute of Fluid Science, Tohoku University. His research interests include various shock wave phenomena, high-speed photography, and flash radiography. He has received seven awards including the coveted Ernst Mach Medal in 2000.

Clean monochromatic x-ray irradiation from weakly ionized linear copper plasma

Eiichi Sato, MEMBER SPIE
Iwate Medical University
Department of Physics
Morioka 020-0015, Japan
E-mail: dresato@iwate-med.ac.jp

Etsuro Tanaka
Tokyo University of Agriculture
Department of Nutritional Science
Faculty of Applied Bioscience
Setagaya-ku 156-8502, Japan

Hidezo Mori
National Cardiovascular Center Research Institute
Department of Cardiac Physiology
Osaka 565-8565, Japan

Toshiaki Kawai, MEMBER SPIE
Hamamatsu Photonics K.K.
Electron Tube Division #2
Iwata-gun 438-0193, Japan

Shigehiro Sato
Iwate Medical University
Department of Microbiology
School of Medicine
Morioka 020-8505, Japan

Kazuyoshi Takayama, MEMBER SPIE
Tohoku University
Shock Wave Research Center
Institute of Fluid Science
Sendai 980-8577, Japan

Abstract. In the plasma flash x-ray generator, a 200-nF condenser is charged up to 50 kV by a power supply, and flash x-rays are produced by the discharging. The x-ray tube is a demountable triode with a trigger electrode, and the turbomolecular pump evacuates air from the tube with a pressure of approximately 1 mPa. Target evaporation leads to the formation of weakly ionized linear plasma, consisting of copper ions and electrons, around the fine target, and intense Kα rays are produced using a 10-μm-thick nickel filter. At a charging voltage of 50 kV, the maximum tube voltage is almost equal to the charging voltage of the main condenser, and the peak current is about 15 kA. When the charging voltage is increased, the linear plasma forms, and the copper Kα intensities substantially increase. The Kα lines are quite clean and intense, and hardly any bremsstrahlung rays are detected at all. The x-ray pulse widths are approximately 700 ns, and the time-integrated x-ray intensity has a value of approximately 20 μC/kg at 1.0 m from the x-ray source with a charging voltage of 50 kV. [DOI: 10.1117/1.1882373]

Subject terms: flash x-ray; weakly ionized linear plasma; copper target; Kα characteristic x-rays; monochromatic x-rays.

Paper 040184 received Mar. 29, 2004; revised manuscript received Sep. 9, 2004; accepted for publication Oct. 25, 2004; published online Mar. 30, 2005. This paper is a revision of a paper presented at SPIE conference on Laser-Generated and Other Laboratory X-Ray and EUV Sources, Optics, and Applications, Aug. 2003, San Diego, California. The paper presented there appears (unrefereed) in SPIE Proceedings Vol. 5196.

1 Introduction

Flash x-rays have been produced by several different methods, and various generators have been developed corresponding to specific radiographic objectives.[1–3] Currently, maximum photon energy has been increased to approximately 1 MeV using multistage Marx pulse generators[1,2] to produce hard x-rays for military studies. In soft x-ray generators,[4–7] high-intensity single generators with large capacity condensers were originally developed. Subsequently, repetitive generators[8–12] have been developed, and the repetition rate has been increased to subkilohertz using a cold-cathode triode.

Recently, soft x-ray lasers have been produced by a gas-discharge capillary,[13–16] and the laser pulse energy substantially increased in proportion to the capillary length. These kinds of fast discharges can generate hot and dense plasma columns with aspect ratios approaching 1000:1. However, it is difficult to increase the laser photon energy to 10 keV or beyond. Because there are no x-ray resonators in the high photon energy region, new methods for increasing coherence will be desired in the future.

0091-3286/2005/$22.00 © 2005 SPIE

We have developed several different plasma flash x-ray generators corresponding to specific radiographic objectives, and a major goal in our research is the development of an intense and clean monochromatic x-ray generator that can impact applications with biomedical radiography. By forming weakly ionized linear plasma,[17–20] because we have succeeded in producing fairly intense and clean quasi-monochromatic x-rays from the plasma axial direction, monochromatic x-rays should be produced using a K-edge filter.

We describe a plasma flash x-ray generator utilizing a new plasma x-ray tube, and used it to perform a preliminary experiment for generating clean monochromatic x-rays by forming a linear copper plasma cloud around a fine target.

2 Generator

2.1 *High-Voltage Circuit*

Figure 1 shows a block diagram of the high-intensity plasma flash x-ray generator. This generator consists of the following essential components: a high-voltage power supply, a high-voltage condenser with a capacity of approximately 200 nF, a turbomolecular pump, a krytron pulse

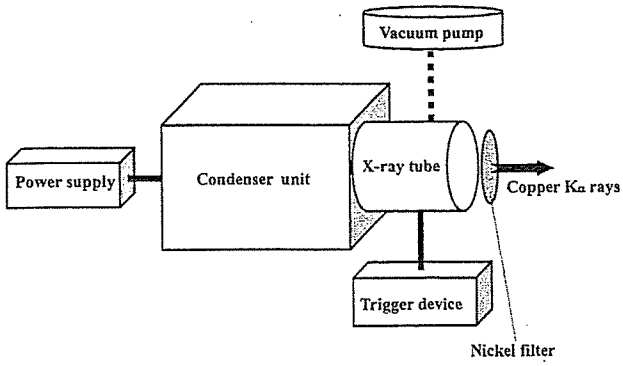

Fig. 1 Block diagram of high-intensity plasma flash x-ray generator.

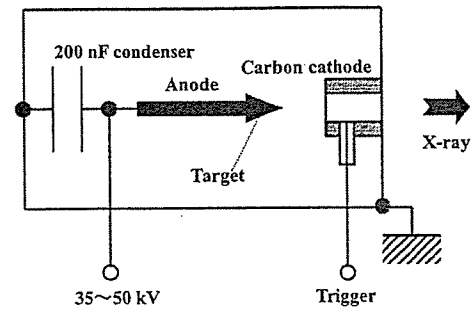

Fig. 2 Circuit diagram of generator.

generator as a trigger device, and a flash x-ray tube. In this generator, a low-impedance transmission line (Fig. 2) is employed to increase maximum tube current. The high-voltage main condenser is charged to 50 kV by the power supply, and electric charges in the condenser are discharged to the tube after triggering the cathode electrode with the trigger device. The plasma flash x-rays are then produced.

2.2 *X-Ray Tube*

The x-ray tube is a demountable cold cathode triode that is connected to the turbomolecular pump with a pressure of approximately 1 mPa (Fig. 3). This tube consists of the following major parts: a hollow cylindrical carbon cathode with a bore diameter of 10.0 mm, a brass focusing electrode, a trigger electrode made from copper wire, a stainless-steel vacuum chamber, a nylon insulator, a polyethylene terephthalate (Mylar) x-ray window 0.25 mm thick, and a rod-shaped copper target 3.0 mm in diameter with a tip angle of 60 deg. The distance between the target and cathode electrodes is approximately 20 mm, and the trigger electrode is set in the cathode electrode. As electron beams from the cathode electrode are roughly converged to the target by the focusing electrode, evaporation leads to the formation of a weakly ionized linear plasma, consisting of copper ions and electrons, around the fine target.

2.3 *Principle of Clean Kα-Ray Irradiation*

In the linear plasma, bremsstrahlung photons with energies higher than the K-absorption edge are effectively absorbed and are converted into fluorescent x-rays (Fig. 4). The plasma then transmits the fluorescent rays easily, and bremsstrahlung rays with energies lower than the K edge are also absorbed by the plasma. In addition, because bremsstrahlung rays are not emitted in the opposite direction to that of electron acceleration, intense characteristic x-rays are generated from the plasma-axial direction. Sub-

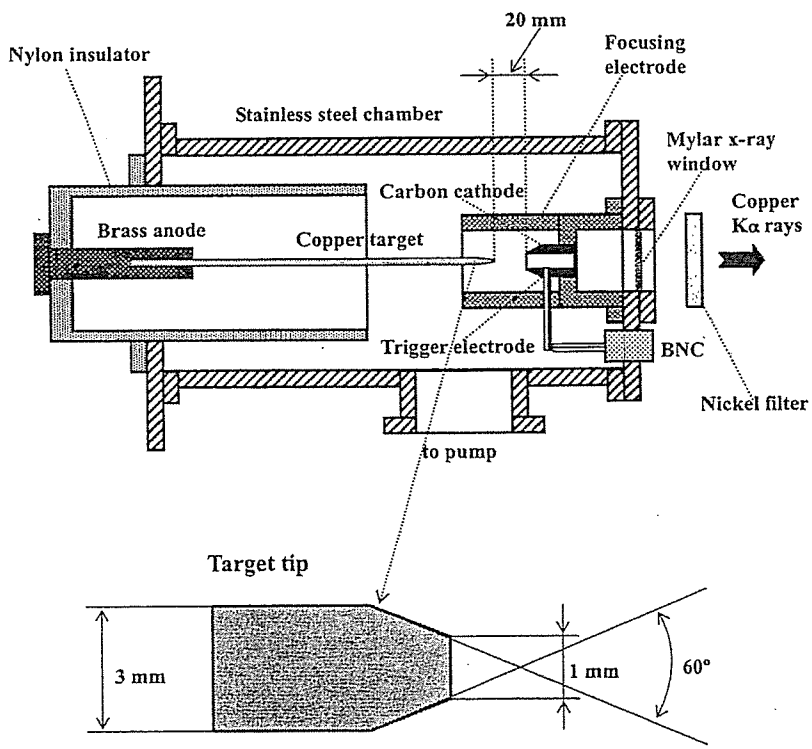

Fig. 3 Schematic drawing of flash x-ray tube with rod target.

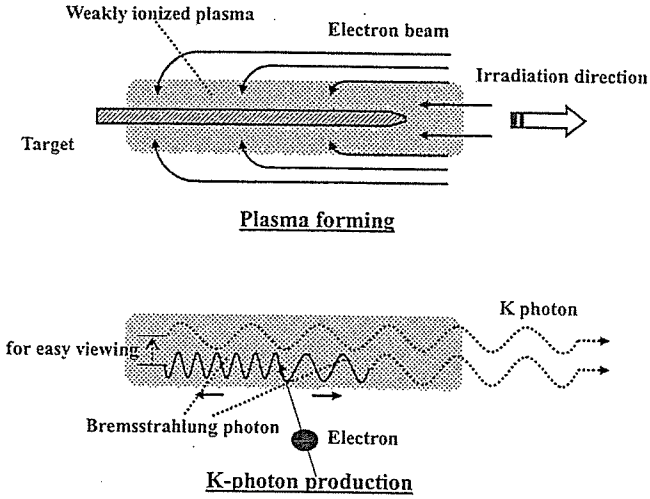

Fig. 4 K-photon irradiation from weakly ionized plasma.

sequently, Kβ rays (8.90 keV) are absorbed effectively using a 10-μm-thick nickel K-edge filter with an edge of 8.33 keV, and quite clean Kα rays (8.04 keV) are produced.

3 Characteristics

3.1 *Tube Voltage and Current*

Tube voltage and current were measured by a high-voltage divider with an input impedance of 1 GΩ and a current transformer, respectively. Figure 5 shows the time relation for the tube voltage and current. At the indicated charging voltages, they roughly displayed damped oscillations. When the charging voltage was increased, both the maximum tube voltage and current increased. At a charging voltage of 50 kV, the maximum tube voltage was almost equal to the charging voltage of the main condenser, and the maximum tube current was approximately 15 kA.

3.2 *X-Ray Output*

An x-ray output pulse was detected using a combination of a plastic scintillator and a photomultiplier using a 10-μm-thick monochromatic copper filter (Fig. 6). The x-ray pulse height substantially increased with corresponding increases in the charging voltage. The x-ray pulse widths were about 700 ns, and the time-integrated x-ray intensity per pulse measured by a thermoluminescence dosimeter (Kyokko TLD Reader 1500 utilizing MSO-S elements without energy compensation) had a value of about 20 μC/kg at 1.0 m from the x-ray source, with a charging voltage of 50 kV.

3.3 *X-Ray Source*

To measure images of the Kα source, we employed a pinhole camera with a hole diameter of 100 μm (Fig. 7). When the charging voltage was increased, the plasma x-ray source grew, and both spot dimension and intensity increased. Because the x-ray intensity is the highest at the center of the spot, both the dimension and intensity decreased according to both increases in the thickness of a filter for absorbing x-rays and decreases in the pinhole diameter.

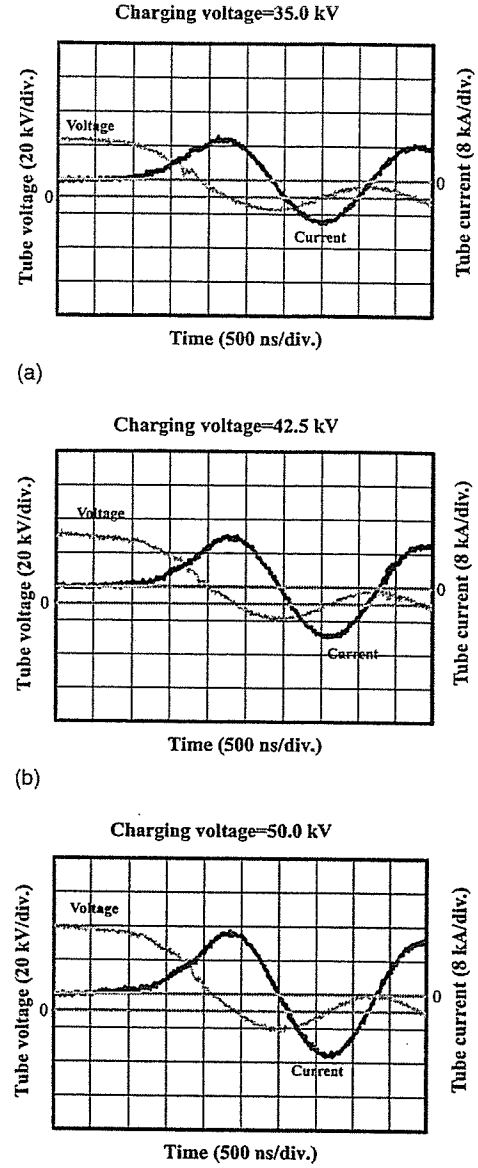

Fig. 5 Tube voltages and currents with charging voltage of (a) 35.0 kV, (b) 42.5 kV, and (c) 50.0 kV.

3.4 *X-Ray Spectra*

X-ray spectra from the plasma source were measured using a transmission-type spectrometer with a lithium fluoride

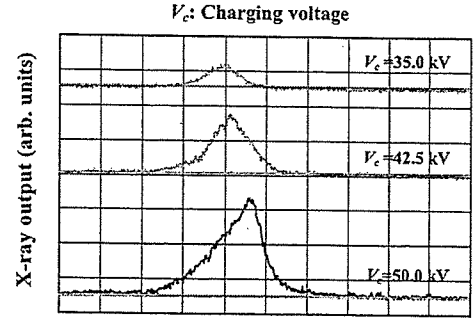

Fig. 6 X-ray outputs measured by plastic scintillator with changes in charging voltage.

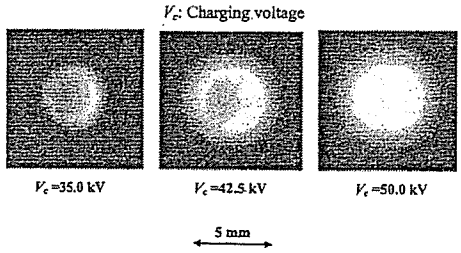

Fig. 7 Images of Kα x-ray source measured by pinhole of 100 μm from plasma axial direction.

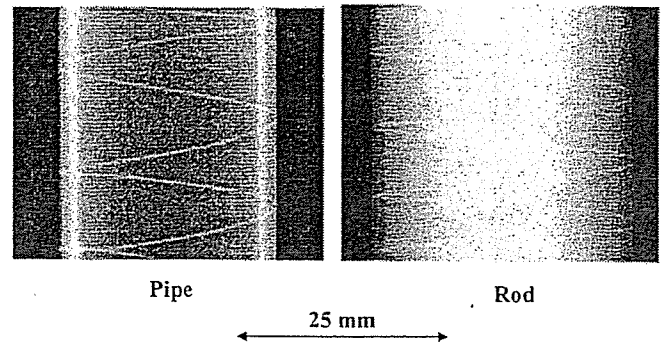

Fig. 9 Radiograms of tungsten wires 50 μm in diameter coiled around pipe, and rod made of polymethyl methacrylate.

curved crystal 0.5 mm in thickness. The spectra were taken by a computed radiography (CR) system[21] (Konica Regius 150) with a wide dynamic range, using the filter, and relative x-ray intensity was calculated from Dicom digital data. Figure 8 shows measured spectra from the copper target using the filter. In fact, we observed clean Kα lines such as lasers, and confirmed the significant filtering effect, while bremsstrahlung rays were hardly detected at all. The characteristic x-ray intensity of the Kα lines substantially increased with corresponding increases in the charging voltage, and the Kβ line was absorbed by the filter. Although this spectrometer has sufficient energy resolution for measuring Kα_1 and Kα_2 lines, we could observe only a single line.

4 Radiography

Plasma radiography was performed by the CR system without using the filter, and the distance between the x-ray source and imaging plate was 1.2 m.

First, rough measurements of image resolution were made using wires. Figure 9 shows radiograms of 50-μm-diam tungsten wires coiled around a pipe, and a rod made of polymethyl methacrylate with a charging voltage of 50 kV. Although the image contrast increased using the pipe, 50-μm-diam wires could be observed.

The image of water falling into a polypropylene beaker from a glass test tube is shown in Fig. 10. This image was taken with a charging voltage of 45 kV, with the slight addition of an iodine-based contrast medium. Because the x-ray duration was about 1 μs, the stop-motion image of water could be obtained.

Figure 11 shows an angiogram of a rabbit heart; iodine-based microspheres of 15 μm in diameter were used with a charging voltage of 50 kV, and fine blood vessels of about 100 μm were visible.

5 Discussion

Concerning the spectrum measurement, we obtained fairly clean Kα lines from a weakly ionized linear plasma x-ray

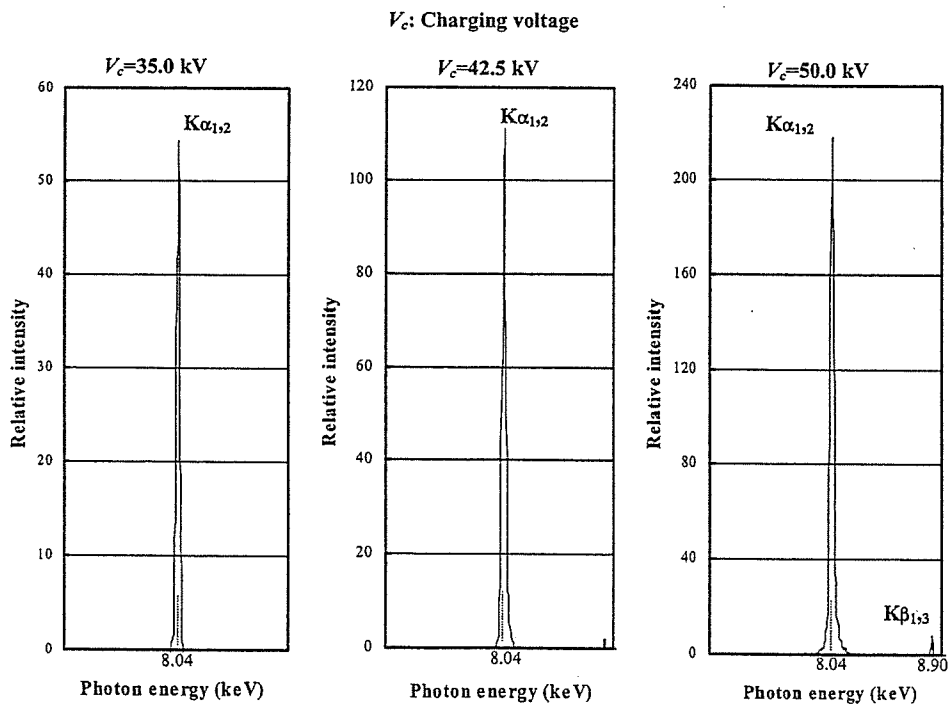

Fig. 8 X-ray spectra from weakly ionized copper plasma according to changes in charging voltage and to insertion of nickel K-edge filter.

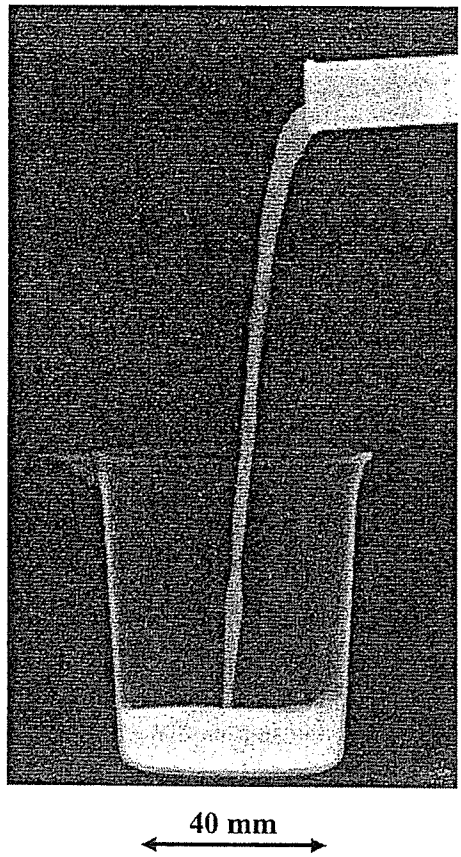

Fig. 10 Radiogram of water falling into polypropylene beaker from glass test tube.

source by absorbing Kβ lines using the K-edge filter. The lines are produced by x-ray enhancement by spontaneous emission, and the coherence can be increased by development of a resonator or by pulse laser irradiations from the plasma axial direction to produce higher harmonics. In a medical application, cerium Kα rays (34.6 keV) are absorbed effectively by an iodine-based contrast medium, and high contrast microangiography can be performed.

In this research, we obtained sufficient characteristic x-ray intensity per pulse for CR radiography using the filter, and the generator-produced number of characteristic Kα photons was approximately 5×10^{13} photons/cm$^2\cdot$s at 1.0 m from the source. In addition, since the photon energy of characteristic x-rays can be controlled by changing the target elements, various quasimonochromatic high-speed

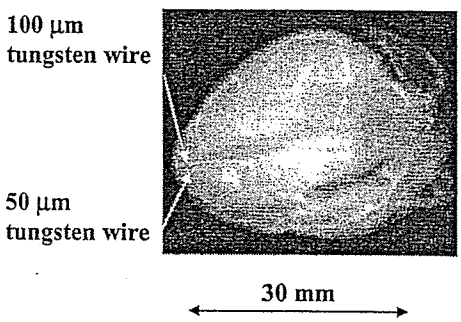

Fig. 11 Angiograms of rabbit heart.

radiographies, such as high-contrast microangiography and parallel radiography using an x-ray lens, will be possible.

Acknowledgments

This work was supported by Grants-in-Aid for Scientific Research (13470154, 13877114, and 16591222) and Advanced Medical Scientific Research from MECSST; Health and Labor Sciences Research Grants (RAMT-nano-001, RHGTEFB-genome-005, and RHGTEFB-saisei-003); and grants from Keiryo Research Foundation, The Promotion and Mutual Aid Corporation for Private Schools of Japan, Japan Science and Technology Agency (JST), and New Energy and Industrial Technology Development Organization (NEDO, Industrial Technology Research Grant Program in 2003).

References

1. A. Mattsson, "Some characteristics of a 600 kV flash x-ray tube," *Phys. Scr.* **5**, 99–102 (1972).
2. R. Germer, "X-ray flash techniques," *J. Phys. E* **12**, 336–350 (1979).
3. C. Cavailler, "AIRIX—a new tool for flash radiography in detonics," *Proc. SPIE* **4183**, 23–35 (2000).
4. E. Sato, H. Isobe, and F. Hoshino, "High intensity flash x-ray apparatus for biomedical radiography," *Rev. Sci. Instrum.* **57**, 1399–1408 (1986).
5. E. Sato, M. Sagae, K. Takahashi, T. Oizumi, H. Ojima, K. Takayama, Y. Tamakawa, T. Yanagisawa, A. Fujiwara, and K. Mitoya, "High-speed soft x-ray generators in biomedicine," *Proc. SPIE* **2513**, 649–667 (1994).
6. E. Sato, M. Sagae, K. Takahashi, A. Shikoda, T. Oizumi, H. Ojima, K. Takayama, Y. Tamakawa, T. Yanagisawa, A. Fujiwara, and K. Mitoya, "Dual energy flash x-ray generator," *Proc. SPIE* **2513**, 723–735 (1994).
7. E. Sato, M. Sagae, A. Shikoda, K. Takahashi, T. Oizumi, M. Yamamoto, A. Takabe, K. Sakamaki, Y. Hayasi, H. Ojima, K. Takayama, and Y. Tamakawa, "High-speed soft x-ray techniques," *Proc. SPIE* **2869**, 937–955 (1996).
8. E. Sato, S. Kimura, S. Kawasaki, H. Isobe, K. Takahashi, Y. Tamakawa, and T. Yanagisawa, "Repetitive flash x-ray generator utilizing a simple diode with a new type of energy-selective function," *Rev. Sci. Instrum.* **61**, 2343–2348 (1990).
9. S. Kimura, E. Sato, M. Sagae, A. Shikoda, T. Oizumi, K. Takahashi, Y. Tamakawa, and T. Yanagisawa, "Disk-cathode flash x-ray tube driven by a repetitive two-stage Marx pulser," *Med. Biol. Eng. Comput.* **31**, S37–S43 (1993).
10. A. Shikoda, E. Sato, M. Sagae, T. Oizumi, Y. Tamakawa, and T. Yanagisawa, "Repetitive flash x-ray generator having a high-durability diode driven by a two-cable-type line pulser," *Rev. Sci. Instrum.* **65**, 850–856 (1994).
11. E. Sato, K. Takahashi, M. Sagae, S. Kimura, T. Oizumi, Y. Hayasi, Y. Tamakawa, and T. Yanagisawa, "Sub-kilohertz flash x-ray generator utilizing a glass-enclosed cold-cathode triode," *Med. Biol. Eng. Comput.* **32**, 289–294 (1994).
12. K. Takahashi, E. Sato, M. Sagae, T. Oizumi, Y. Tamakawa, and T. Yanagisawa, "Fundamental study on a long-duration flash x-ray generator with a surface-discharge triode," *Jpn. J. Appl. Phys.* **33**, 4146–4151 (1994).
13. J. J. Rocca, V. Shlyaptsev, F. G. Tomasel, O. D. Cortazar, D. Hartshorn, and J. L. A. Chilla, "Demonstration of a discharge pumped table-top soft x-ray laser," *Proc. Phys. Lev. Lett.* **73**, 2192–2195 (1994).
14. J. J. Rocca, D. P. Clark, J. L. A. Chilla, and V. N. Shlyaptsev, "Energy extration and achievement of the saturation limit in a discharge-pumped table-top soft x-ray amplifier," *Phys. Lev. Lett.* **77**, 1476–1479 (1996).
15. C. D. Macchietto, B. R. Benware, and J. J. Rocca, "Generation of millijoule-level soft-x-ray laser pulses at a 4-Hz repetition rate in a highly saturated tabletop capillary discharge amplifier," *Opt. Lett.* **24**, 1115–1117 (1999).
16. J. J. G. Rocca, J. L. A. Chilla, S. Sakadzic, A. Rahman, J. Filevich, E. Jankowska, E. C. Hammarsten, B. M. Luther, H. C. Kapteyn, M. Murnane, and V. N. Shlyapsev, "Advances in capillary discharge soft x-ray laser research," *Proc. SPIE* **4505**, 1–6 (2001).
17. E. Sato, Y. Suzuki, Y. Hayashi, E. Tanaka, H. Mori, T. Kawai, K. Takayama, H. Ido, and Y. Tamakawa, "High-intensity quasi-monochromatic x-ray irradiation from the linear plasma target," *Proc. SPIE* **4505**, 154–164 (2001).
18. E. Sato, Y. Hayasi, E. Tanaka, H. Mori, T. Kawai, T. Usuki, K. Sato, H. Obara, T. Ichimaru, K. Takayama, H. Ido, and Y. Tamakawa,